

# Analysis of high energy resolution data of $^{26}\text{Mg}(^3\text{He},t)^{26}\text{Al}$ reaction

Kalayar Win <sup>1,\*</sup>, Yoshitaka Fujita <sup>2,3</sup>, Yee Yeeoo <sup>4</sup> and Hiro Fujita <sup>2</sup>

<sup>1</sup> Department of Physics, Pakokku University, Pakokku, Myanmar

<sup>2</sup> Research Center for Nuclear Physics, Osaka University, Osaka 567-0047, Japan

<sup>3</sup> Department of Physics, Osaka University, Osaka 560-0043, Japan

<sup>4</sup> Taungoo University, Taungoo, Myanmar

**Abstract.** The Gamow-Teller (GT) transition is a powerful tool to study nuclear structure because of its simple form of the operator  $\sigma\tau$ . The structure of  $^{26}\text{Al}$  is studied through Gamow-Teller transitions using nuclear charge-exchange reaction. The reaction  $^{26}\text{Mg}(^3\text{He},t)^{26}\text{Al}$  was performed at an incident energy of 140 MeV/nucleon and scattering angle at and near  $0^\circ$ . The energy resolution of  $\Delta E = 22$  keV allowed us to study many discrete states. Most of the prominent states are suggested that they are excited with  $\Delta L = 0$  GT transitions. The GT states were studied up to 18.5 MeV. For the extraction of the B(GT) value, the proportionality between cross section and B(GT) was used. The standard B(GT) values were obtained from the  $^{26}\text{Si}$  beta decay, where the mirror symmetry of B(GT) was obtained. The  $T = 2$  GT states are expected in the region  $E_x \geq 13.5$  MeV. By comparing with the results of  $^{26}\text{Mg}(t, ^3\text{He})^{26}\text{Na}$  reactions, the isospin symmetry of  $T = 2$  GT states is discussed. Due to the high-energy resolution, the decay widths  $\Gamma$  for the states in the  $E_x > 9$  MeV region could be studied. The narrow width of the  $T = 2$  states at 13.592 MeV is explained in terms of isospin selection rules.

## 1 Introduction

Gamow-Teller transitions are mediated by the spin-isospin ( $\sigma\tau$ ) interaction. They are characterized by an angular momentum transfer  $\Delta L = 0$  and spin-isospin flip ( $\Delta S = 1$  and  $\Delta T = 1$ ). Due to this simple character, GT transitions are important tools for the study of nuclear structure [1-6]. Studies of  $\beta$  decay give the most direct information on the reduced GT transition strength B(GT); an absolute B(GT) value can be derived. However, the excitation energy ( $E_x$ ) accessible in a  $\beta$  decay is limited by the decay Q value. In addition, there is a rapid decrease in feeding as  $E_x$  increases owing to the decrease in the phase-space factor [3, 5]. In charge-exchange reactions such as the (p, n), ( $^3\text{He}$ , t), (n, p) and (t,  $^3\text{He}$ ), one can observe GT transitions to states at higher excitation energies without the Q-value limitation.

In the charge-exchange reactions, states excited by GT transitions (GT states) become prominent at intermediate incident energies (above 100 MeV/nucleon) and forward angles around  $0^\circ$ . This is because of the  $\Delta L = 0$  nature of the GT transitions and the dominance of the  $\sigma\tau$  part of the effective nuclear interaction at small momentum transfer  $q$  [7, 8]. Under

\*e-mail: 009.kalayar@gmail.com

these experimental conditions it was found that there is a close proportionality between the GT cross sections and the B(GT) values [7, 8],

$$\sigma^{GT}(q, \omega) \simeq K(\omega) N_{\sigma\tau} |J_{\sigma\tau}(q)|^2 B(GT) \quad (1)$$

$$= \hat{\sigma}^{GT} F(q, \omega) B(GT), \quad (2)$$

where  $J_{\sigma\tau}(q)$  is the volume integral of the effective interaction  $V_{\sigma\tau}$  at momentum transfer  $q$  ( $\approx 0$ ),  $K(\omega)$  is the kinematic factor,  $\omega$  is the total energy transfer, and  $N_{\sigma\tau}$  is a distortion factor. The value  $\hat{\sigma}^{GT}$  is the unit cross section for the GT transition at  $q = \omega = 0$  and a given incoming energy for a system with mass number  $A$ . The  $F(q, \omega)$  value gives the dependence of the GT cross sections on the momentum and energy transfers. It takes a value of unity at  $q = \omega = 0$  and usually decreases gradually as a function of  $E_x$ , and can be obtained from distorted-wave Born approximation (DWBA) calculations.

In order to obtain detailed structural information on  $^{26}\text{Al}$ , we investigate GT transitions from the  $T_z = +1$  nucleus  $^{26}\text{Mg}$  leading to GT states up to  $E_x = 18.5$  MeV in the  $T_z = 0$  nucleus  $^{26}\text{Al}$  using a (p, n) type ( $^3\text{He}$ , t) reaction at 140 MeV/nucleon, where  $T_z$  is the z component of isospin  $T$  defined by  $(N-Z)/2$ . By improving the dispersion matching techniques, we could realize a higher-energy resolution of  $\Delta E = 22$  keV (FWHM) in the  $^{26}\text{Mg}(^3\text{He}, t)^{26}\text{Al}$  reaction. Excitation of many GT states could be studied. In particular, in the  $E_x = 8.5$ -12 MeV region, we could observe a concentration of fragmented GT states. The strengths of them are distributed like a resonance structure. Note that this is the region where Gamow-Teller resonances (GTRs) are expected [4, 5]. The higher energy resolution also allows us to derive decay widths of states in the GTR region. We found that many states in the  $E_x > 9$  MeV region are noticeably broader than the experimental energy resolution. It is note that the proton separation energy  $S_p$  in  $^{26}\text{Al}$  is 6.31 MeV. And these states can make proton decay.

Fig. 1 shows the isospin analogous structure and the isospin analogous GT transitions in the  $A = 26$  isobars. As can be seen,  $T_z = \pm 1 \rightarrow 0$  GT transitions studied in the  $^{26}\text{Mg}(^3\text{He}, t)^{26}\text{Al}$  reaction and the  $^{26}\text{Si}$   $\beta$  decay to  $^{26}\text{Al}$  are analogous under the assumption of isospin symmetry and thus we can assume that these transitions have the same B(GT) values. Since absolute B(GT) values can be obtained from  $^{26}\text{Si}$  beta decay, we use the  $\beta$  decay B(GT) values up to 2.74 MeV for the derivation of the unit GT cross section  $\hat{\sigma}^{GT}$ . The B(GT) values for the transitions to higher excited states can be derived using close proportionality given in Eq. 2. As illustrated in Fig. 1, the ( $^3\text{He}$ , t) reaction can excite  $T = 0, 1$  and  $2, J^\pi = 1^+$  GT states in the  $T_z = 0$  nucleus  $^{26}\text{Al}$  starting from the  $T = 1, J^\pi = 0^+$  ground state of the  $T_z = +1$  nucleus  $^{26}\text{Mg}$ , where  $T = 2$  analogous states are situated in the high-energy region. On the other hand, (n, p) charge exchange reactions such as (t,  $^3\text{He}$ ) reaction can excite only  $T = 2$  analogous states situated in low-energy region of  $T_z = +2$  nucleus  $^{26}\text{Na}$ .

## 2 Experiment

The  $^{26}\text{Mg}(^3\text{He}, t)^{26}\text{Al}$  experiment, was performed at the Research Center for Nuclear Physics (RCNP), Osaka University by using a 140 MeV/nucleon  $^3\text{He}$  beam from the K = 400 Ring Cyclotron and high-resolution type magnetic spectrometer, Grand-Raiden [12]. The measurement was performed by setting the spectrometer at  $0^\circ$ . The  $^3\text{He}$  beam bombarded a self-supporting  $^{26}\text{Mg}$  target having the areal density of  $0.87$  mg/cm<sup>2</sup> and the isotopic enrichment of 99.4%. A thin target foil was used because the difference of the atomic energy losses of  $^3\text{He}^{2+}$  and the triton in the target causes the energy spread of the outgoing triton. The beam was stopped by a Faraday cup placed inside the first dipole magnet of Grand Raiden and the beam current was measured and integrated.

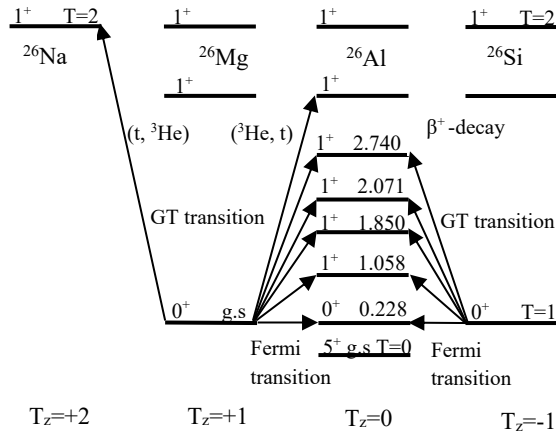


Fig. 1. Schematic view of the isospin analogous states and analogous GT transitions in the  $A=26$ ,  $T_z=+2$ ,  $+1$ ,  $0$  and  $-1$  isobars

The outgoing tritons were momentum analyzed within the full acceptance of the spectrometer and were focused at the focal plane detector system consisting of a multiwire drift chamber and two thin plastic detectors allowed for particle identification and track reconstruction. The acceptance of the spectrometer was subdivided into five angle cuts using the information of tracks. The full energy-range spectrum for the scattering cut of  $\theta \leq 0.5^\circ$  is shown in Fig. 2.

In order to accurately determine the scattering angle  $\Theta$  around  $0^\circ$  angle measurements in both  $x$  direction ( $\theta$ ) and  $y$  direction ( $\phi$ ) are equally important, where  $\Theta$  is defined by  $\Theta = \sqrt{\theta^2 + \phi^2}$ . Good  $\theta$  and  $\phi$  resolutions were achieved by applying angular dispersion matching technique and the over-focus mode in the spectrometer respectively. The  $^{26}\text{Mg}$  target used in the experiment contained a small amount of the  $^{24}\text{Mg}$  isotope ( $\approx 0.5\%$ ). In order to identify the  $^{24}\text{Al}$  states in the  $^{26}\text{Al}$  spectrum, if existing, we compared our  $^{26}\text{Al}$  spectrum with that of the  $^{24}\text{Al}$  measured in the  $^{24}\text{Mg}(^3\text{He}, t)^{24}\text{Al}$  reaction under the same experimental

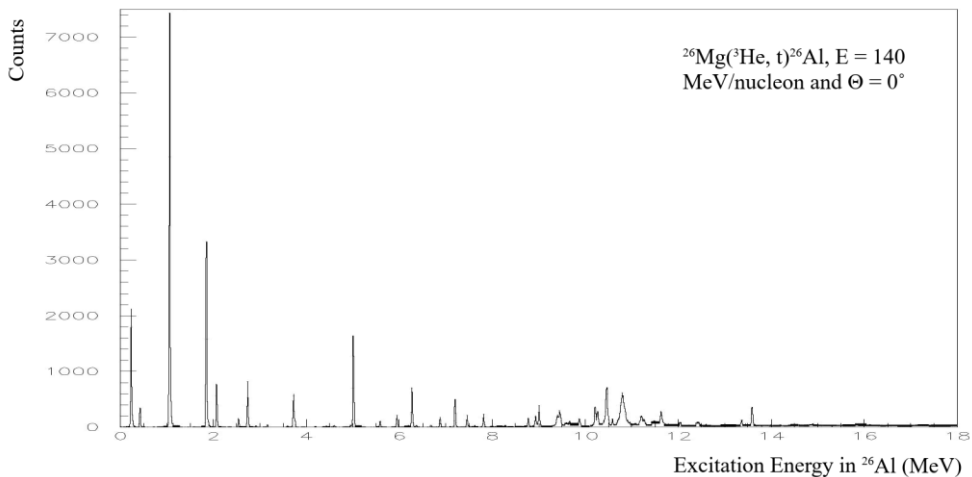


Fig. 2 The full count and full range spectrum of the  $^{26}\text{Mg}(^3\text{He}, t)^{26}\text{Al}$  reaction.

conditions. In our  $^{26}\text{Al}$  spectrum, we did not find  $^{24}\text{Al}$  peaks corresponding to the strongly excited  $1^+$  GT states. The energy spectrum of the  $^{26}\text{Mg}(^3\text{He}, t)^{26}\text{Al}$  reaction  $E_x$  up to 9 MeV

and the energy spectrum of the  $E_x$  between 9 MeV and 19 MeV are shown in Fig. 3 and 4 respectively.

### 3 Data analysis

The acceptance of the  $0^\circ$  setting of the spectrometer was subdivided into five angle cuts of  $\Theta \leq 0.5^\circ$ ,  $0.5^\circ-0.8^\circ$ ,  $0.8^\circ-1.2^\circ$ ,  $1.2^\circ-1.6^\circ$  and  $1.6^\circ-2.0^\circ$  by doing a software analysis. For each spectrum generated by the angle cuts, peak positions, and yields of the observed states were obtained using the peak-fitting program S-FIT [13], in which the shape of the well separated peak at 1.058 MeV was used as a reference. Above the  $S_p$  value of 6.31 MeV, continuum caused by the quasi-free scattering reaction can appear. In the spectrum, the continuous counts become noticeable above  $E_x \approx 8.5$  MeV and gradually increase with the excitation energy. Therefore, a smooth empirical background connecting the deepest valleys between peaks was subtracted in the peak-fit analysis. The peak counts in  $\Theta \leq 0.5^\circ$  spectrum are given column 6 of Table 1 and column 3 of Table 2 for  $E_x = 0-8$  MeV region and 8-12 MeV region, respectively.

In addition, in the  $E_x > 9.4$  MeV region, i.e., the region more than 3 MeV higher than  $S_p$ , it was found that many states are broader than the lower-lying states due to the decay width. The decay width of each state was derived assuming a Breit-Wigner shape of the broadening using the program S-FIT. Since our energy resolution is 22 keV, we estimate that the minimum decay width that can be extracted is  $\approx 10$  keV. The obtained widths  $\Gamma$  are given in column 5 of Table 2 for states with good statistics.

#### 3.1 Excitation energy

The  $E_x$  values of  $J^\pi = 1^+$  GT states in  $^{26}\text{Al}$  have been evaluated within uncertainties of 1 keV up to 7.880 MeV state in Ref. [11]. The  $E_x$  values of higher excited states were determined with the help of kinematic calculations from their peak positions in the  $\Theta \leq 0.5^\circ$  spectrum. In order to obtain the relationship between the peak positions in the spectrum and the corresponding values of magnetic rigidity of the spectrometer, we took a calibration spectrum for a natural magnesium ( $^{\text{nat}}\text{Mg}$ ) target. This target was thin ( $\approx 1.5$  mg/cm<sup>2</sup>) and spectrum was taken under the same experimental conditions as for the  $^{26}\text{Mg}$  target. The reaction Q values for the isotopes  $^{26}\text{Mg}$  and  $^{24}\text{Mg}$  are different by about 10 MeV in the ( $^3\text{He}$ , t) measurements (about 4.0 MeV and 13.9 MeV respectively). The  $E_x$  values of a few low-lying states in  $^{24}\text{Al}$  up to 1.090 MeV are known with accuracy better than 1 keV. In addition, the  $E_x$  values of higher excited states in  $^{24}\text{Al}$  up to  $E_x \approx 6.5$  MeV were determined in a  $\beta^+$ -decay study of  $^{24}\text{Si}$ , although the uncertainties were larger ( $\approx 12$  keV). Therefore, all  $E_x$  values of  $^{26}\text{Al}$  states up to  $E_x \approx 16.5$  MeV could be determined by interpolation.

We estimate that the uncertainties of the obtained  $E_x$  values are 1-2 keV up to  $E_x \approx 9$  MeV for the states having more than  $\approx 500$  counts. As can be seen in the Table 1, we are in good agreement up to  $E_x = 7.8$  MeV with the value given in Ref. [10], where precise  $E_x$  values are also in good agreement up to 9 MeV with those listed in Ref. [9]. Most of the states in the region between 9-14 MeV have decay widths. Therefore, we estimate uncertainties of  $\leq 8$  keV for the well isolated peaks with good statistics.

For the states in the region between 14 and 16.5 MeV, we estimate larger uncertainties of 10-20 keV. In this region, the peak widths are larger and the statistics lower, and thus the peak decomposition analysis has a larger uncertainty. Since the  $E_x$  value of the highest observed state, i.e., 18.5 MeV, was determined by extrapolation, we estimate an uncertainty of  $\approx 30$  keV. Above this energy, no sharp peak was observed. The  $E_x$  values of states determined in the achromatically tuned ( $^3\text{He}$ , t) reaction [10] are given in columns 8 and 6 of Tables 1 and 2, respectively.

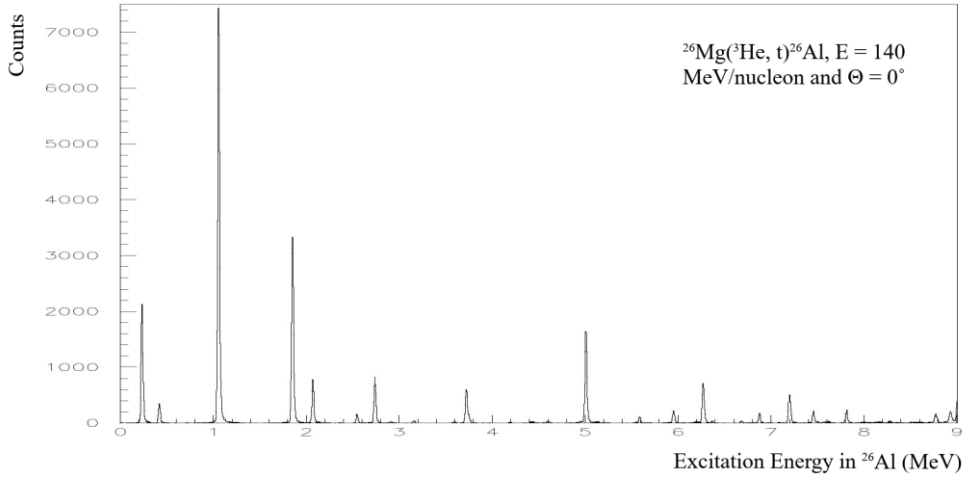


Fig. 3 The energy spectrum of the  $^{26}\text{Mg}(^3\text{He}, t)^{26}\text{Al}$  reaction  $E_x$  up to 9 MeV

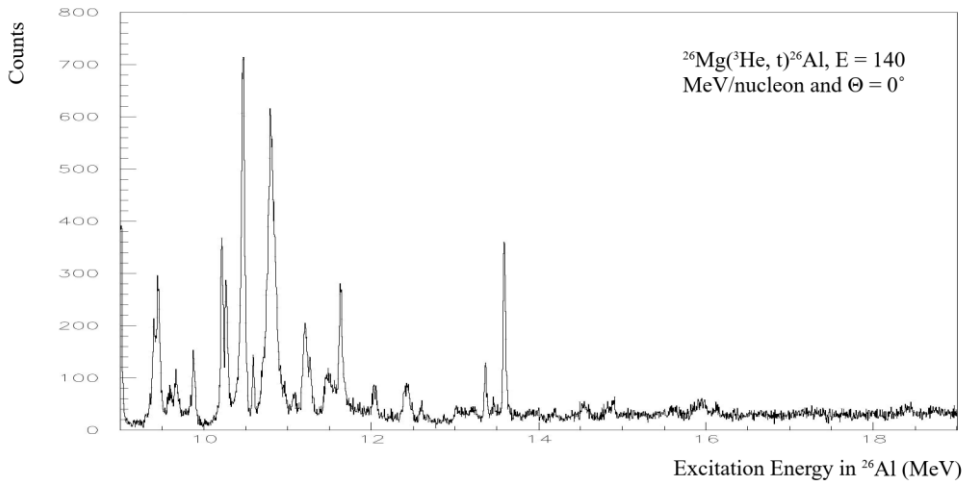


Fig. 4 The energy spectrum of the  $^{26}\text{Mg}(^3\text{He}, t)^{26}\text{Al}$  reaction  $E_x$  between 9 MeV and 19 MeV

### 3.2 Assignment of angular momentum transfer

Due to the  $\Delta L = 0$  nature of the GT excitation, it is expected that a GT state has the largest intensity at  $0^\circ$  and smaller intensities at larger angle. On the other hand, states with  $\Delta L \geq 1$  have larger intensities at large angles. In order to identify the candidates for GT states having such  $\Delta L = 0$  nature, relative peak intensities of each state in the five spectra for the different angle cuts mentioned above were examined, where the reference was taken from the prominent 1.058 MeV state, the most strongly excited  $J^\pi = 1^+$  GT state.

Many state well excited in the  $\Theta \leq 0.5^\circ$  spectrum showed relative peak intensities similar to those of the reference peak, suggesting that they are excited with  $\Delta L = 0$ . On the other hand, weakly excited states in the  $\Theta \leq 0.5^\circ$  spectrum mostly showed the larger peak intensities within  $\approx 20\%$  compared to those of the reference peak in the five angle cuts was accepted as a  $\Delta L = 0$  excitation. For the weakly excited states and also for the states in the higher  $E_x$  region, the  $\Delta L = 0$  assignments were less clear.

Table 1. States of  $^{26}\text{Al}$  up to 8 MeV, GT transition strengths B(GT) and Counts

Evaluated values [11]			$(^3\text{He}, t)$ present work				$(^3\text{He}, t)$ [10]	
$E_x$ (MeV)	$J^\pi$	$\beta$ -decay B(GT)	$E_x$ (MeV)	$\Delta L$	Counts ( $0^\circ$ )	B(GT)	$E_x$ (MeV)	B(GT)
0.0	$5^+$		0.0	$\geq 1$	46(8)			
0.2283	$0^+$		0.230	0	10563(137)			
1.0577	$1^+$	1.098(26)	1.057	0	38041(264)	1.089(26)	1.06	1.090(30)
1.8506	$1^+$	0.526(12)	1.850	0	18639(183)	0.536(14)	1.85	0.540(20)
2.0716	$1^+$	0.088(05)	2.070	0	4072(87)	0.117(04)	2.07	0.114(08)
2.7400	$1^+$	0.110(05)	2.740	0	3959(85)	0.115(04)	2.74	0.119(08)
3.7238	$1^+$		3.724	0	3392(208)	0.099(06)	3.73	0.109(08)
5.0102	$1^+$		5.010	0	9132(128)	0.271(07)	5.01	0.280(10)
5.9499	$1^+$		5.951	0	1218(48)	0.036(02)	5.94	0.041(05)
6.2702	$1^+$		6.269	0	4178(90)	0.126(04)	6.27	0.134(08)
6.8743	$1^+$		6.876	0	882(41)	0.027(01)	6.87	0.028(04)
7.1984	$1^+$		7.199	0	2785(72)	0.085(03)	7.20	0.089(06)
7.4553	$1^+$		7.457	0	1096(47)	0.034(02)	7.46	0.036(04)
7.8136	$1^+$		7.815	0	1199(49)	0.037(02)	7.81	0.037(04)

The result of the  $\Delta L$  assignment is shown in column 5 and 2 of Table 1 and 2, respectively. Note that most of the prominent states in Figs. 3 and 4 are assigned as  $\Delta L = 0$ . It is note that the  $(^3\text{He}, t)$  reaction at 140 MeV/ nucleon is strongly selective for the  $\Delta L = 0$  excitation in the measurement at  $0^\circ$ . The 0.228 MeV peak assigned as the isobaric analog state (IAS) of the g.s. of  $^{26}\text{Mg}$  also shows a  $\Delta L = 0$  character. It is expected that the Fermi strength is concentrated in the single transition to this IAS. Accordingly, we assume that all states populated in  $\Delta L = 0$  transitions, except the IAS, are GT states.

In comparison with the achromatically tuned  $(^3\text{He}, t)$  reaction [10], it was found that both experiments are in agreement for the assignments of  $\Delta L = 0$  states up to  $E_x = 8$  MeV. However, in the higher  $E_x$  region, we see that some of our states are doublets. Owing to the good energy resolution, many weakly excited states could be observed in the lower  $E_x$  region of  $< 8.5$  MeV.

### 3.3 Evaluation of B(GT) values

Counts of individual states in the  $\Theta \leq 0.5^\circ$  angle cut obtained in the peak-decomposition analysis are shown as ‘Counts ( $0^\circ$ )’ in Tables 1 and 2. The reduced transition strength B (GT) is derived for each  $\Delta L = 0$  state using this value and the close proportionality given by Eq. (2). In order to use this relationship, we need reference B(GT) value(s) and have to derive unit counts for the unit B(GT). First, we rely on isospin symmetry in isobars. As can be seen in Fig. 1, GT transitions in the  $T_z = -1 \rightarrow 0$   $\beta$  decay from the  $0^+$  g.s. of  $^{26}\text{Si}$  and the  $T_z = +1 \rightarrow 0$   $^{26}\text{Mg}(^3\text{He}, t)^{26}\text{Al}$  reaction reaching to the same low-energy  $1^+$  states in  $^{26}\text{Al}$  are analogous (mirror GT transitions). We assume that B(GT) values are equal for a pair of analogous GT transitions. In  $\beta$  decay, the reduced GT strength  $B_j(\text{GT})$  for the GT transition to the  $j^{\text{th}}$  state is expressed using the  $ft$  value as

$$B_j(\text{GT})\lambda^2 = K/f_j t_j, \quad (3)$$

Table 2. States of  $^{26}\text{Al}$  in the  $E_x = 8.5\text{-}18.5$  MeV region and GT transition strengths  $B(\text{GT})$ . The results from the present and achromatically tuned  $^{26}\text{Mg} (^3\text{He}, t) ^{26}\text{Al}$  reactions are compared.

$(^3\text{He}, t)$ present work					$(^3\text{He}, t)$ [10]	
$E_x$ (MeV)	$\Delta L$	Counts ( $0^\circ$ )	B(GT)	$\Gamma$ (keV)	$E_x$ (MeV)	B(GT)
8.934	0	1698(60)	0.053(02)			
					8.98	0.123(08)
9.008	0	2355(71)	0.074(03)			
9.403	0	2517(109)	0.079(04)	31(6)		
					9.43	0.136(08)
9.454	0	3109(113)	0.098(04)	28(6)		
					9.86	0.058(06)
9.878	0	1747(71)	0.056(03)	38(5)		
10.213	0	3090(94)	0.099(04)	13(2)		
					10.24	0.158(09)
10.267	0	2265(89)	0.073(03)	18(2)		
10.464	0	8494(138)	0.273(08)	25(5)	10.45	0.290(10)
10.590	0	878(109)	0.028(03)			
10.802	0	14840(190)	0.480(13)	69(8)	10.81	0.470(20)
11.208	0	2537(94)	0.083(04)	40(7)		
					11.22	0.164(09)
11.268	0	1270(79)	0.041(03)	23(5)		
11.476	0	1620(180)	0.053(06)	(48)	11.50	0.021(05)
11.560	(0)	569(140)	0.019(04)			
11.636	0	3365(105)	0.111(04)	24(6)	11.62	0.170(10)
11.690	(0)	547(73)	0.018(02)			

Where  $K = 6143.6(17)$ ,  $\lambda = g_A/g_B = -1.270(3)$ ,  $f_j$  is the  $\beta$ -decay phase-space factor calculated using the decay Q value, and  $t_j$  is the partial half-life. Using the  $\log ft$  values obtained in the  $^{26}\text{Si}$   $\beta$ -decay [11], the  $B(\text{GT})$  values could be derived for the four GT transitions to low-lying states in  $^{26}\text{Al}$  applying Eq. (3). The calculated values are listed in column 3 of Table 1. The  $B(\text{GT})$  values of other GT states were calculated using the close proportionality given in Eq. (2). In order to evaluate the  $E_x$  dependence of  $F(q, \omega)$ , a DWBA calculation was performed for the  $^{26}\text{Mg}(^3\text{He}, t)^{26}\text{Al}$  reaction using the computer code DW81 [14] following the procedure described in Refs. [15-17]. The optical potential parameters were taken from Ref. [18].

In order to obtain the unit cross section of  $B(\text{GT})$ , we selected two largest  $\beta$ -decay  $B(\text{GT})$  values of 1.098(26) and 0.526(12) for the transitions to the 1.058 MeV and 1.581 MeV states, respectively. By using this unit cross-section, a good agreement has been achieved for the corresponding  $B(\text{GT})$  values in the  $\beta$ -decay and the present  $(^3\text{He}, t)$  reaction, which suggests that the close proportionality in Ref.[7] works for these GT transitions to the low-lying states. In the  $(^3\text{He}, t)$  reaction performed at an intermediate energy of 140 MeV/nucleon, states excited with  $\Delta L = 0$  transitions are most probably GT states [5]. Therefore,  $B(\text{GT})$  values are calculated for all  $\Delta L = 0$  states. The obtained  $B(\text{GT})$  values are given in column 7 of Table 1 and column 4 of Table 2.

## 4 Discussion

### 4.1 Fine structure of states in the Gamow-Teller resonance region

In Tables 1 and 2, results from the present work are compared with those from the achromatically tuned ( $^3\text{He},t$ ) reaction [10]. As mentioned, good agreement are seen up to  $E_x = 8$  MeV, while some differences are observed in the GTR region of  $E_x \approx 8-12$  MeV. We see in Table 2 that the state observed at 8.98 MeV in Ref. [10] is now resolved into two states at 8.934 and 9.008 MeV. We found that both of them are excited with  $\Delta L = 0$  and the sum of their B(GT) values is comparable to that of the 8.98 MeV state in Ref. [10].

In a similar way, the 9.43 MeV state is now resolved into the 9.403 MeV and 9.45 MeV states, and the 10.24 MeV state into the 10.213 MeV and 10.267 MeV states, and 11.22 MeV state into 11.208 MeV and 11.268 MeV states, where the sums of our B(GT) values all correspond to the B(GT) values given in Ref. [10] within their error bars. In the  $E_x = 11.4-11.7$  MeV region, we observed four states. In Ref. [10] only two states were recognized at 11.50 MeV and 11.62 MeV. However, the total B(GT) strength is again about the same. Therefore, the total B(GT) strength is redistributed into the four states at 11.476, 11.560, 11.636 and 11.690 MeV.

It can be seen that GT strength concentrates in two energy regions. About 58% of the observed strength is in the region below  $E_x \approx 8$  MeV and about 38% of the strength is in the energy region of 8-12 MeV, i.e. the GTR region. Above this region, one sharp state at 13.592 MeV and four weakly excited states were identified as GT states.

### 4.2 $T = 2$ Gamow-Teller states in $^{26}\text{Al}$ and $^{26}\text{Na}$

The target nucleus  $^{26}\text{Mg}$  has the isospin value  $T_i = 1$ . Due to the  $\Delta T = 0, \pm 1$  nature of the  $\sigma$  (GT) operator,  $T_f = 0, 1$  and 2 GT states in  $^{26}\text{Al}$  are excited in the  $^{26}\text{Mg}(^3\text{He}, t)^{26}\text{Al}$  reaction. On the other hand, in the (n, p) type CE reactions, only the  $T_f = 2$  GT states are excited in the final nucleus  $^{26}\text{Na}$  owing to their  $T_z = +2$  nature [5]. Therefore, a pair of states that are commonly observed in the high  $E_x$  region of  $^{26}\text{Al}$  and the low  $E_x$  region of  $^{26}\text{Na}$  can be isospin analogous states with  $T=2$ .

The states in the  $E_x > 13.5$  MeV region observed in the achromatically tuned  $^{26}\text{Mg}(^3\text{He}, t)^{26}\text{Al}$  measurement were compared with the low-lying states observed in the (n, p) type  $^{26}\text{Mg}(t, ^3\text{He})^{26}\text{Na}$  reaction at  $E_t = 115$  MeV/nucleon [10]. It was suggested that the states observed at 13.57 MeV and higher energies in  $^{26}\text{Al}$  are candidates for the  $T = 2$  states. Among them, it was identified that the 13.57 MeV state was the analog state of the  $J^\pi = 1^+, 0.08$  MeV state in  $^{26}\text{Na}$ .

#### 4.2.1 Gamow-Teller transition strengths to the $T = 2$ states

Let us examine the difference of B(GT) values in a pair of isospin analogous GT transition starting from  $T = 1$  g.s. of  $^{26}\text{Mg}$  ( $T_z = +1$ ). First we see that the squared value of isospin Clebsch-Gordan (CG) coefficient for a GT transition to a  $T = 2$  GT state in  $^{26}\text{Na}$  ( $T_z = +2$ ) is unity. On the other hand, the one to the analog GT state in  $^{26}\text{Al}$  ( $T_z = 0$ ) is 1/6. Therefore, it is expected that the B(GT) value to a  $T = 2$  state obtained in  $\beta^+$ -type  $^{26}\text{Mg} \rightarrow ^{26}\text{Na}$  reactions is six times larger than the one obtained in  $\beta^-$ -type  $^{26}\text{Mg} \rightarrow ^{26}\text{Al}$  reactions. Thus, in order to make a direct comparison with the B(GT<sup>+</sup>) values from the  $\beta^+$ -type (t,  $^3\text{He}$ ) reaction, the B(GT) values from the  $\beta^-$ -type ( $^3\text{He}, t$ ) reactions given in Table 2 ought to be multiplied by a factor 6. These modified values are listed in Table 3. Good agreement of B(GT<sup>-</sup>) and B(GT<sup>+</sup>) values is seen for GT transitions from the g.s. of  $^{26}\text{Mg}$  to the pair of analog states at

13.592 MeV in  $^{26}\text{Al}$  and at 0.08 MeV in  $^{26}\text{Na}$ . Reasonable agreement is also apparent for the other three pairs of excited states.

### 4.3 Decay widths of states

For the states above the proton separation energy  $S_p = 6.31$  MeV, proton decay becomes possible. Since the proton decay is a fast process, lifetimes of states can be short, and thus states can have a decay width  $\Gamma$ . The  $\Gamma$  value is small in the region just above  $S_p$  owing to the Coulomb barrier, while a larger width is expected at higher  $E_x$  regions. We could derive decay widths for the states in the GTR region (see column 5 of Table 2). Here, we try to interpret the feature of the observed decay widths for the states in the GTR region and also for the 13.592 MeV,  $T = 2$  state.

Table 3. Candidates of GT states in the  $E_x = 13.5\text{-}18.5$  MeV region in  $^{26}\text{Al}$  and in the  $E_x \leq 5.5$  MeV region in  $^{26}\text{Na}$ .

$(^3\text{He}, t)$ present work		$(^3\text{He}, t)$ [10]		$(t, ^3\text{He})$ [10]		$^{26}\text{Na}$ states
$E_x$ (MeV)	B(GT)	$E_x$ (MeV)	B(GT)	$E_x$ (MeV)	B(GT)	$E_x$ (MeV)
13.592 [0.08]	0.41(2)	13.57	0.41(2)	0.08	0.42(3)	0.082(1)
14.54 [1.03]	0.11(1)	14.53	0.09(2)			
14.90 [1.39]	0.08(1)	14.88	0.11(3)	1.4(2)	0.09(2)	1.509(1)
15.96 [2.45]	0.13(3)	15.91	0.17(4)	2.6(2)	0.13(2)	2.720(3)
18.43 [4.92]	0.12(2)	18.32	0.13(6)	5.1(4)	0.22(4)	

#### 4.3.1 Decay width of the 13.592 MeV, $T = 2$ state

In the higher  $E_x$  region, an interesting observation is made; the 13.592 MeV,  $T = 2$  state is sharp and its peak width is not appreciably broader than the ones of the states in the low-lying region. We find that the narrow peak width of this  $T = 2$  state can be explained in terms of isospin selection rules in the proton decay of a  $^{26}\text{Al}$  state. Consider the proton decay of a  $T = 0$  or 1 state in  $^{26}\text{Al}$ . It can be seen from the selection rules that both  $T = 0$  and  $T = 1$  state can decay into a proton with  $T = 1/2$  and a low lying  $^{25}\text{Mg}$  state having  $T = 1/2$  and  $E_x$  ( $T = 1/2$ ), if the  $E_x$  values of the initial states in  $^{26}\text{Al}$  exceed  $S_p + E_x$  ( $T = 1/2$ ), i.e.,  $6.31 + E_x$  ( $T = 1/2$ ) MeV.

On the other hand, a  $T = 2$  state in  $^{26}\text{Al}$  can decay only into a proton and a  $T = 3/2$  state in  $^{25}\text{Mg}$ , where the lowest  $T = 3/2$  state in  $^{25}\text{Mg}$  is situated relatively high (at  $E_x = 7.79$  MeV). Therefore, the proton decay of  $T = 2$  states in  $^{26}\text{Al}$  is allowed only for the states located higher than  $S_p + E_x$  ( $T = 3/2$ ), i.e.,  $6.31 + 7.79 = 14.10$  MeV. Therefore, the 13.592 MeV,  $T = 2$  state, in principle, cannot make proton decay and is kept sharp. In reality, however, isospin  $T$  is not a good quantum number and a small amount of impurity is expected. Therefore, what we can say is that the proton decay of 13.592 MeV,  $T = 2$  state is suppressed and its decay width  $\Gamma$  is  $\leq 10$  keV, i.e., the experimental detection limit.

## 5. Summary

In summary, GT excitations were studied by the  $^{26}\text{Mg}(^3\text{He}, t)^{26}\text{Al}$  reaction at 140 MeV/nucleon and at  $0^\circ$ . At an energy resolution of 22 keV, many fragmented states were observed. Many of the prominent states were excited with  $\Delta L = 0$  excited states and the

known  $J^\pi = 1^+$  GT states up to 8 MeV, indicating that the ( $^3\text{He}$ , t) reaction is sensitive to GT excitation. The GT states in  $^{26}\text{Al}$  by interpolation up to  $\approx 17$  MeV.

The GT transition strengths, the B(GT) values, were derived assuming the close proportionality between cross sections and B(GT) values. The reference B(GT) value was obtained from the  $^{26}\text{Si}$   $\beta$ -decay measurements, where the mirror symmetry between  $T_z = \pm 1 \rightarrow 0$  GT transitions was assumed. The GT strength was mainly distributed in two energy regions, i.e., the lower  $E_x$  region of  $< 8.5$  MeV and the GTR region of  $E_x = 8\text{-}12$  MeV, where about 58% of the observed strength was found in the lower  $E_x$  region.

Starting from the  $T = 1$  g.s. of  $^{26}\text{Mg}$ , the (p, n) type ( $^3\text{He}$ , t) reaction can excite GT states with  $T = 0, 1$  and  $2$  in  $^{26}\text{Al}$ . On the other hand, (n, p) type charge exchange reactions excite only the  $T = 2$  states in  $^{26}\text{Na}$ . Note that the GT transitions from the ground state of  $^{26}\text{Mg}$  to the  $T = 2$  states in  $^{26}\text{Al}$  and  $^{26}\text{Na}$  are analogous. We compared the B(GT) values of the analogous transitions to the  $T = 2$  GT states in  $^{26}\text{Al}$  and  $^{26}\text{Na}$  obtained, respectively, in the present  $^{26}\text{Mg}(^3\text{He}, t)^{26}\text{Al}$  reaction and in the  $^{26}\text{Mg}(t, ^3\text{He})^{26}\text{Na}$  reaction. After a proper correction of the geometrical factors, it was found that the B(GT) values in these (p, n) and (n, p) type CE reactions were the same within the experimental uncertainties.

Owing to the high energy resolution achieved in the  $^{26}\text{Mg}(^3\text{He}, t)^{26}\text{Al}$  reaction, we could observe the larger peak widths for discrete states in the GTR region of  $E_x \approx 9\text{-}12$  MeV. Since these states are situated above the proton separation energy  $S_p = 6.31$  MeV, it is suggested that these states are broader due to the decay width. Proton decay widths could be derived for these discrete GT states. The peak width of the 13.592 MeV,  $T = 2$  GT state situated more than 7 MeV above  $S_p$ , however, was not apparently broader than the experimental resolution, suggesting that the proton decay is suppressed. The suppression of the proton decay can be understood in terms of the isospin selection rule that disallows proton decay of  $T = 2$  states below  $E_x = 14.1$  MeV.

First of all, the author thanks the organization of International Symposium Multi-particle Dynamics, for the organizers allow writing this paper in EPJ. The author also thanks RCNP as the ( $^3\text{He}$ , t) experiments were performed at RCNP, Osaka University, Japan.

## References

- [1] A. Bohr and B.R. Mottelson, *Nuclear Structure* (Benjamin, New York, 1969), Vol. 1.
- [2] F. Osterfeld, *Rev. Mod. Phys.* **64**, 491 (1992).
- [3] B. Rubio and W. Gelletly, *Lect. Notes Phys.* **764**, 99 (2009).
- [4] J. Rapaport and E. Sugarbaker, *Ann. Rev. Nucl. Part. Sci.* **44**, 109 (1994).
- [5] Y. Fujita, B. Rubio, and W. Gelletly, *Prog. in Part. and Nucl. Phys.* **66**, 549 (2011).
- [6] K. Langanke and G. Martinez-Pinedo, *Rev. Mod. Phys.* **75**, 819 (2003).
- [7] T. N. Taddeucci *et al.*, *Nucl. Phys. A* **469**, 125 (1987).
- [8] W. G. Love, K. Nakayama, and M. A. Franey, *Phys. Rev. Lett.* **59**, 1401 (1987).
- [9] Y. Fujita *et al.*, *Phys. Rev. C* **67**, 064312 (2003).
- [10] R. G. T. Zegers *et al.*, *Phys. Rev. C* **74**, 024309 (2006).
- [11] M. S. Basunia and A. M. Hurst, *Nucl. Data Sheets* **134**, 1 (2016).
- [12] M. Fujiwara *et al.*, *Methods Phys. Res. A* **422**, 484 (1999).
- [13] H. Fujita *et al.*, RCNP (Osaka University), Annual Report, 2010, p. 3.
- [14] DW 81, a DWBA computer code by J. R. Comfort (1981) and updated version (1986), an extended version of DWBA 70 by R. Schaeffer and J. Raynal (1970).
- [15] S. Y. van der Werf *et al.*, *Nucl. Phys. A* **496**, 305 (1989).
- [16] R. Schaeffer, *Nucl. Phys. A* **164**, 145 (1971).
- [17] R. G. T. Zegers, *et al. Phys. Rev. Lett.* **90**, 202501 (2003).
- [18] T. Yamagata *et al.*, *Nucl. Phys. A* **589**, 425 (1995).